Article

An Application of Machine Learning Algorithms by Synergetic Use of SAR and Optical Data for Monitoring Historic Clusters in Cypriot Cities

Maria Spyridoula Tzima [1,*], **Athos Agapiou** [2], **Vasiliki Lysandrou** [2], **Georgios Artopoulos** [3,*], **Paris Fokaides** [4] **and Charalambos Chrysostomou** [1]

1 Computation-Based Science and Technology Research Center, The Cyprus Institute, Nicosia 2121, Cyprus; c.chrysostomou@cyi.ac.cy
2 Earth Observation Cultural Heritage Research Lab, Department of Civil Engineering & Geomatics, Cyprus University of Technology, Limassol 3036, Cyprus; athos.agapiou@cut.ac.cy (A.A.); vasiliki.lysandrou@cut.ac.cy (V.L.)
3 Science and Technology in Archaeology and Culture Research Center, The Cyprus Institute, Nicosia 2121, Cyprus
4 School of Engineering, Frederick University, Nicosia 1036, Cyprus; eng.fp@frederick.ac.cy
* Correspondence: m.tzima@cyi.ac.cy (M.S.T.); g.artopoulos@cyi.ac.cy (G.A.)

Abstract: In an era of rapid technological improvements, state-of-the-art methodologies and tools dedicated to protecting and promoting our cultural heritage should be developed and extensively employed in the contemporary built environment and lifestyle. At the same time, sustainability principles underline the importance of the continuous use of historic or vernacular buildings as part of the building stock of our society. Adopting a holistic, integrated, multi-disciplinary strategy can link technological innovation with the conservation and restoration of heritage buildings. This paper presents the ongoing research and results of the application of Machine Learning methods for the remote monitoring of the built environment of the historic cluster in Cypriot cities. This study is part of an integrated, multi-scale, and multi-disciplinary study of heritage buildings, with the end goal of creating an online HBIM platform for urban monitoring.

1. Introduction

Historic urban environments are not given static formations that are disconnected from the contemporary fabric of a city, but rather a set of tangible and intangible assets subject to the dynamic pressures of economic, environmental, and social activities. Looking beyond important historic cities previously preserved by authorities, numerous second- and third-tier cities have grown from their historic centres due to prior urbanisation phenomena. However, they have faced various difficulties in safeguarding and integrating heritage buildings into the contemporary fabric of the city in a sustainable way. Examples of such cities challenged by gentrification, depopulation, and neglect can be found in Cyprus, Greece, South Italy, and elsewhere. Monitoring the pressures caused by the aforementioned city-wide phenomena on historic clusters can prove helpful for local authorities to prevent future losses of building stock. Different stakeholders and professionals have used onsite analysis and Earth Observation methods separately. However, remote sensing and computational tools have recently enabled the large-scale, real-time monitoring of cities.

Developing built heritage digitisation methods should focus on expanding the scope of study beyond the individual buildings and allowing for a deeper understanding and interdisciplinary interpretation of said building's condition and performance within its topographical context and the surrounding built environment. This could become a reality

today using the advancements in remote sensing, algorithms, and the computation prowess of hardware available to researchers. Expanding the scale and area of focus of heritage studies to enable reuse of heritage can benefit from studies that look beyond the scale of the building asset. Looking at the urban context can provide researchers, professionals, and the relevant stakeholders with new insights into chronological urban studies through methods that have been previously very resourceful and difficult to implement computationally. The proliferation of digital methods and tools for creating digital twins of cities [1], as well as the research contributing to the area of City Information Modelling, all demonstrate the need for represented information to be handled on both a neighbourhood and city scale.

Nowadays, as the Earth Observation data volume is growing, the need to transform this raw data into valuable products is highly required. In addition, the value of land cover and land use monitoring has increased to understand the frequent environmental changes and address the challenges of specific environmental problems. In this context, this study demonstrates a user-friendly methodology that extracts meaningful information from multi-temporal Copernicus Sentinel-1 and Sentinel-2 images to map urban growth while recording details about the spatial changes.

The paper draws on the ongoing research and intermediate results of the project "Portal for heritage buildings integration into the contemporary built environment" (PERIsCOPE) (https://uperiscope.cyi.ac.cy/, accessed on 30 March 2023), which is co-financed by the European Regional Development Fund and the Republic of Cyprus.

This paper begins with a literature review, followed by the aim of the research, the objectives, and the description of the case study areas. Following this, Section 6, with the title "Method: Remote Sensing Analysis at Neighbourhood Scale," outlines the methodology and the data used in the study. Then, experiments and a detailed analysis of the results are given in Section 4. Lastly, the discussion and conclusions are presented in Sections 5 and 6, respectively.

2. Materials

International literature has mainly been mainly concerned with the recent rapid increase in the urbanisation of cities. The concept of smart cities appears to meet the challenges of urbanisation and be an appropriate strategy to address the difficulties of urban sustainability. The three main pillars of the smart city concept seem to be the IoT, big data, and theoretical analyses, including several application fields, numerous implemented case studies, and citizen-related aspects [2]. As pointed out by Yarashynskaya and Prus [3], the role of smart energy solutions is crucial for a proper Smart City function. It is grounded on the escalating demand for energy in urban areas, as well as the importance of energy in the development of other key Smart City sectors, such as manufacturing, construction, and housing. However, Adibhesami et al. [4] declared that the effect of sustainable energy policies on human physical and mental health should be examined when making decisions in this domain.

Many studies have been conducted to map urban growth results and understand the Earth's Land Usage and Land Cover (LULC) chronologically by modeling the changes that occur owing to artificial structures and natural phenomena. For instance, Bakr et al. [5] declared that change detection of LULC using multi-temporal satellite image data provided effective methods and accurate results to estimate the interaction between human activities and natural phenomena. Furthermore, Pesaresi et al. [6] presented an automatic recognition of human settlements in arid regions with scattered vegetation, using the multispectral Quick Bird satellite dataset. In their research, Rong et al. [7] analysed the driving factors of land use carbon emissions in the area of the lower Yellow River, which has experienced rapid industrialisation and urbanisation, with drastic land use changes from 1995–2018. Jadraque Gago et al. [8] applied the Maximum Likelihood classifier to produce land cover maps that examine the relationship between the pattern of the urban fabric and the formation and evolution of the Surface Urban Heat Island (SUHI).

Remote sensing techniques have been broadly applied to build environment monitoring. The substantial increase in satellite imagery provides a large amount of data support for deep learning methods in urban monitoring and, subsequently, the opportunity to explore various approaches in the field of remote sensing analysis. For instance, Chen et al. [9] proposed a neural network-based method for extracting different Urban Green Spaces (UGS) types, such as parks, using Sentinel-2 images and crowdsourced geospatial big data. Verde et al. [10] used Sentinel-1 and PlanetScope imagery to model the essential land use components required for calculating Sustainable Development Goal (SDG) 11 indicators over the Athens metropolitan area, employing deep learning techniques. To detect building changes, Liu et al. [11] presented a technique in which shape and spatial features were used to improve the discriminability between buildings and other ground objects. Also, Luo et al.'s research focused on building extraction from remote sensing images, by reviewing the most commonly used deep learning methods [12]. Change detection techniques are currently in an advanced stage and have been used to acquire land cover change information for a wide range of applications related to environmental monitoring. Li et al. [13] examined pre-processing techniques to identify newly constructed structures using differences between two Sentinel-1 imageries of Nanjing City. This study used Synthetic-Aperture Radar (SAR) images due to their ability to penetrate cloud cover, as well as their insensitivity to atmospheric and lighting conditions. Papadomanolaki et al.'s [14] research presented a deep-learning architecture for urban change detection using the Onera Satellite Change Detection dataset (OSCD). The proposed method combines a U-Net architecture with Long Short-Term Memory (LSTM) blocks.

In this context, a widely used tool is Sentinel Application Platform (SNAP) [15], a standard, open-source operational platform dedicated to Sentinel data exploitation. For instance, Tsolakidis and Vafiadis [16] used this software to study the urban land cover characteristics of Thessaloniki, Greece, in this software. In their methodology, they applied the Random Forest classifier in both optical Sentinel-2 and radar Sentinel-1 images. Moreover, Radudu et al. [17] used Sentinel-1 products for three years (2016–2019) to analyse the dynamics of the Bucharest's urban population, using change detection techniques in SNAP. SNAP's change detection process has also been applied in other scientific fields. For example, in their research (2017), Sreechanth S and Kiran Yarrakula [18] used the SNAP platform for flood inundation mapping. In their study, the Support-Vector Machine (SVM) classification was performed to map flooded regions and existing water bodies, wherein the changes were detected by the image differencing method.

The protection and preservation of cultural heritage and historical sources is a topic that has garnered a lot of research attention, especially in Europe. A survey focused on presenting a clearer picture of the potential and challenges that can occur during the implementation of fuel-free approaches for projects within a historic city centre was conducted by Simeone et al. [19]. Chahardowli et al.'s paper thoroughly analyses urban regeneration as a multifaceted strategy for revitalizing cities' historic cores. They point out that sustainable regeneration is the outcome of the interaction of four physical, economic, social, and cultural components that support the revitalisation of historic urban clusters [20]. Lastly, occupied with the region of Cyprus, Agapiou [21] used optical and radar data to map the vegetation cover in the vicinity of archaeological sites and landscapes, such as "Nea Paphos" and the "Tombs of the Kings."

Generally, computational techniques – specifically machine learning – can be used to process large amounts of data, with numerous applications in various scientific and engineering fields. Multiple linear regression was applied in Iranmanesh et al.'s study [22], to develop a three-parameter correlation to estimate biomass heat capacity, considering bio-sample chemistry and operating condition. Understanding the complex dynamic behaviours through the use of neural network algorithms has been a centre of interest for researchers such as Roshani et al. [23], who monitor the density and velocity of fluids in the oil and petroleum industries, as well as for Qing et al. [24], who integrated theoretical and experimental data to develop a three-dimensional (3D) model of kerogen. Finally,

intracorporeal suturing – which is one of the crucial hands-on tasks in Fundamentals of Laparoscopic Surgery (FLS) training – is monitored by Mohaidat et al.'s [25] autonomous skill evaluation system, using a variety of one-stage object detectors, including YOLOv4, Scaled-YOLOv4, YOLOR, and YOLOX.

3. Method: Remote Sensing Analysis at Neighbourhood Scale

The research argues that by leveraging multi-scale knowledge with the support of digital tools, such as Supplementary Material S2, it is possible to establish more accurate monitoring strategies for authorities and critical city stakeholders. This in turn helps them prioritise relevant policies and incentives for the sustainable management and development of historic clusters in cities. The presented application of machine learning methods in remote sensing datasets of urban environments in Cyprus was developed to assist authorities through the use of a platform that integrates 3D GIS data from the Cyprus Land and Survey Department. The platform also incorporates 3D models of the specific building blocks under study. These datasets become accessible via an online platform that enables multi-scale monitoring of heritage buildings by means of remote sensing, as well as three-dimensional and reality-captured representations of the built environment. Specifically, this online platform relies on an agile workflow that involves the following steps:

(a) Initial urban scale monitoring of built environment transformations, which may be induced by natural or human activities. By utilising a semi-automated workflow that compares remote sensing data from different time periods, changes in annotated assets within the built environment can be identified. This approach offers a rapid method for connecting large-scale urban phenomena to on-site building observation studies and hypotheses.

(b) Climatic analysis of the site: a contextual survey of the conditions of the built environment surrounding the heritage buildings under study through remote sensing. This study concerns information about the local environment, climatic and topographic conditions of the area at the neighbourhood scale, as well as the assessment of changes in environmental conditions, chronologically.

(c) The survey stage: This includes a conservation state analysis based on non-destructive, diagnostic investigations of building structure and degradation (material, structural, morphological). The analysis includes assessments of hygrothermal properties, decay phenomena, and crack patterns, as well as the use of visual and textual interpretations to identify moisture presence, while documenting and classifying possible causes behind it.

(d) The next stage of the multi-scale advanced survey includes the direct study of the building: e.g., topometric and photographic survey, as well as analysis of formal, constructive, and material aspects. For example, this includes Terrestrial Laser Scanning and photogrammetric surveys of the building, to produce the 3D point-cloud models to be used in the Heritage-Building Information Modelling (HBIM). This also supports the conservation state analysis, providing the accurate information needed for any energy upgrade, retrofit or intervention.

This paper will focus on the first step of the process, which concerns the initial urban scale monitoring of built environment transformations. Through remote sensing monitoring, and onsite analytical digital tools and methodologies, this data-driven observation of historical buildings would enable relevant stakeholders to monitor the built environment and identify risks, such as decay, neglect, or pressures from real estate development and urbanisation that may cause change in the building stock over time. In order to support this aim, the presented research pursues the following objectives to enable remote sensing monitoring of the built environment under study:

(1) As many studies have focused on detecting change with a visual interpretation of the outputs, the proposed methodology addresses the need for combinational approaches. It does this by integrating robust supervised land cover classification procedures with coherent log-likelihood and image differencing change detection techniques. This

combination transforms the results into meaningful insights into the urban landscape. To this end, the key advantages of using Sentinel-1 and Sentinel-2 images, as well as automatic, supervised, and unsupervised machine learning algorithms provides key advantages including time reduction, flexibility in data exploration with multiple solutions, and multilevel similarity modelling.

(2) The analysis of open-access radar and optical products using freely available platforms such as SNAP, QGIS, and Google Earth encourages open data usage in urban planning. As the use of open software is highly promoted in research, the employment of the above tools ensures inclusive workflows and interoperability, contributing to the literature.

The two pilot study areas (Figure 1) of the research were carefully selected to allow a comparative understanding of the impact of environmental change and climatic conditions on building assets. Hence the two clusters studied are located in two urban environments in different climatic zones with varying seismic activity, in Limassol and Nicosia (located in seismic zone 3 and 2, respectively) [26] Specifically, the testbed areas are the historic cluster of Strovolos in Nicosia, and examples in the old city and Turkish-Cypriot quarter of Limassol. Old Strovolos covers an area of approximately 50 hectares, with a population of around 2500 inhabitants (2011 census). The majority of these inhabitants are of Cypriot origin and are settled in around 1000 dwellings. The neighbourhood is a part of the Strovolos Municipality Urban Area, which is the second largest municipality of Cyprus, with a total population exceeding 70,000 inhabitants. The Turkish Cypriot quarter under study in Limassol covers an area of approximately 35 hectares, with a population of around 1400 inhabitants (2011 census). This includes Greek Cypriot refugees and economic emigrants of various origins, all of whom have settled in approximately 500 dwellings. This is a part of the Limassol Municipality Urban Area, which is the largest municipality of Cyprus, with a total population of over 100,000 inhabitants. The chosen study area is covered by ascending and descending passes of Sentinel-1 SAR images and Sentinel-2 multispectral images.
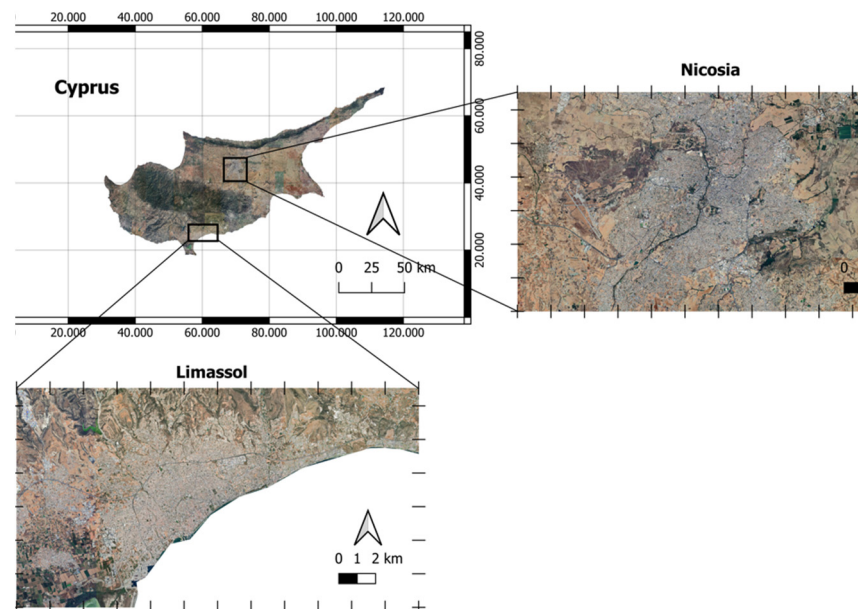

Figure 1. Cyprus and the Areas of Interest (satellite images).

3.1. Data Collection

SAR images and optical data are used to monitor and analyse the urban fabric of the cities of Cyprus. The Sentinel-1 and Sentinel-2 satellite images were downloaded using the Copernicus Open Access Hub (https://scihub.copernicus.eu/dhus, accessed on 25 January

2023) operated by the European Space Agency (ESA). The Sentinel-1 mission performs dual-polarisation C-band SAR imaging acquired at a global scale, with a revisit period of six days. The Sentinel-2 mission supplies optical information ranging from visible to near and medium infrared, with a spatial resolution between 10m and 20m, and a revisit period between five to ten days [27].

Specifically, the two Sentinel-1 Ground Range Detected – High Resolution (GRDH) images were acquired on 6 October 2016 and 29 September 2022, in Interferometric Wide Swath Mode (IW). Detailed properties of the data are shown in Table 1. In order to devise a strategy for the operational exploitation of both radar and optical data in the frame of urban mapping, Sentinel-2 data were also required. In an ideal process, the images of both sensors should be acquired at the same time. To ensure that each pixel's information refers to the same state of the Earth's surface, the duration between the two imagees produced should be reduced to a minimum. Subsequently, for the classification application, a margin of 1 month from the sensing date of the Sentinel-1 image was used to select the corresponding optical image. Moreover, since this kind of image based documentation is prone to show the clouds that cover the Earth's surface, cloud-free images were selected for the purpose of this study. Thus, the Sentinel-2 Level 2A image was acquired on 25 October 2022, with a descending orbit direction and with a cloud cover percentage of 0.41%. Lastly, as no Level 2A products were available for the target area in 2016, the Level 1C image was used for the change detection. So, for the analysis of Limassol, the Sentinel-2 Level 1C image has a sensing date of 16 October 2016, and the area of Nicosia has a sensing date of 8 November 2022.

Table 1. SAR Data specifications.

Date of Dataset	Sensor	Product Type	Sensor Mode	Polarization	Orbit Direction
6 October 2016	Sentinel-1A	GRD	IW	VV + VH	descending
29 September 2022	Sentinel-1A	GRD	IW	VV + VH	descending

Additionally, Open Street Map [28] labelled datasets were used to train the supervised classifiers, and Google Earth data were used for accuracy assessment and the visual interpretation of the results.

3.2. Sentinel-1 Images Pre-Processing

Before using the Sentinel-1 products, applying identical pre-processing procedures to all the scenes was necessary. Pre-processing and analysis of the images was conducted in SNAP software (v9.0.0). SNAP is a scientific image-processing toolbox for Earth Observation studies [29]. During the image pre-processing, several procedures were carried out. Figure 2 summarises the methodological steps of the pre-processing analysis of Sentinel-1 SAR data. The workflow diagram was created in draw.io software (v21.1.2).

Co-polarisation (VV) is used in this study because of its higher sensitivity to urban structures (Figure 3). A subset is required in order to limit the loaded data to the area of interest, minimise errors and speed up processing. In the case of the presented research, this subset was the capital of Cyprus, Nicosia, and the surrounding area. The next step is removing thermal noise using the noise Look-Up Table (LUT) file provided for each product. Radiometric calibration is critical to collocate radar images of various dates, sensors, or imaging geometries. Using a digital elevation model (DEM) to correct SAR geometric errors, Geometric Correction geocodes the image and creates a map-projected output [30]. Additionally, a logarithmic function is applied to the images via the conversion to dB scale, resulting in the normal distribution of the backscatter intensity. Following an evaluation of the available filters (Figure 4), the final phase of pre-processing was the improvement of image quality by speckle filtering. After the speckle filter comparison step, the Lee Sigma filter was selected since it preserves edges and eliminates the haziness of the image [31]. The final products are the calibrated, orthorectified imageries.
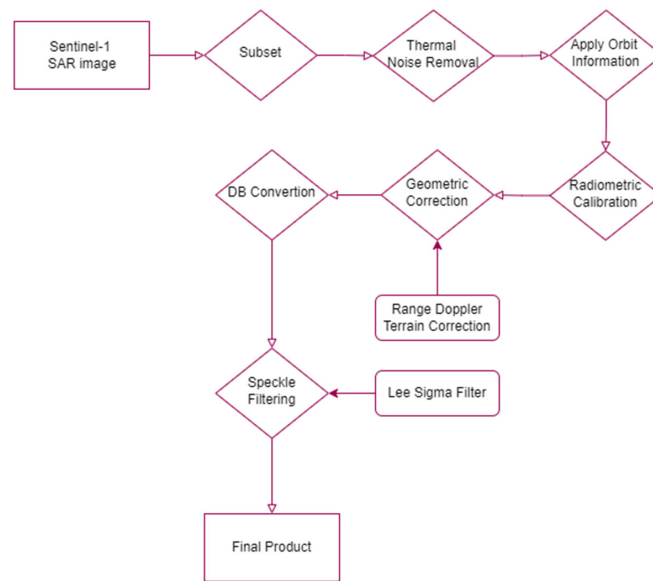
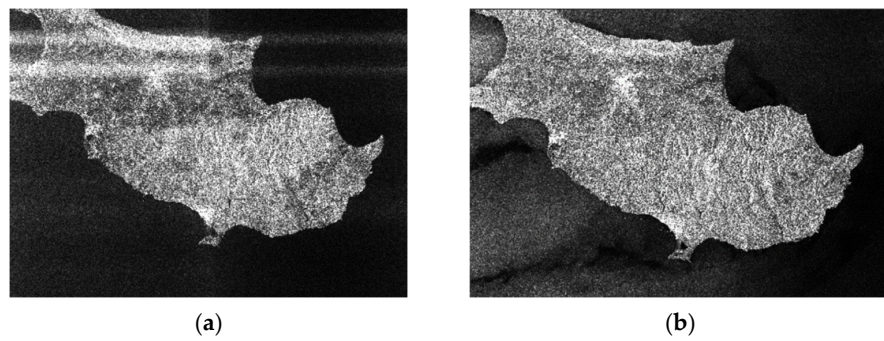**Figure 2.** Pre-processing workflow of SAR images.

Figure 3. Comparison of intensities of Sentinel-1 product with dual polarization, (**a**) Vertical-Horizontal (VH) and (**b**) Vertical-Vertical (VV).
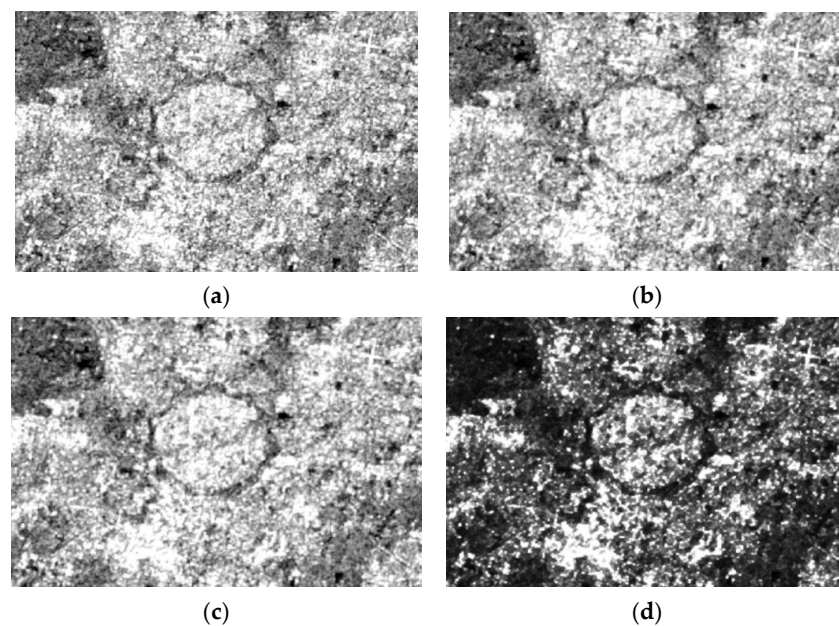

Figure 4. Speckle filtering comparison: (**a**) Lee Sigma; (**b**) Lee; (**c**) Frost; (**d**) Refined Lee.

3.3. Sentinel-2 Images Pre-Processing

Pre-processing procedures and calibrations are also necessary for the optical data to work properly with the images. The following diagram (Figure 5) summarises all of the steps in the pre-processing chain. For Sentinel-2 Level-1C products, the first step of the analysis is the implementation of the Senc2Cor processor. Sen2Cor is a Level-2A generator whose primary purpose is to correct Sentinel-2 Level-1C Top-of-Atmosphere (TOA) data from single-date atmospheric influences, to deliver a Level-2A Bottom-of-Atmosphere (BOA) reflectance product [32]. As the dataset consists of Level-2A images at this point, the next step is the creation of a subset, with the use of spectral bands. Lastly, as not all bands in the Sentinel-2 product have the same resolution, combining some bands during the exploration could cause issues. To combat this, the resampling step is fundamental, and it was applied with the use of B2 as the reference band and the nearest neighbour technique as the upsampling method.
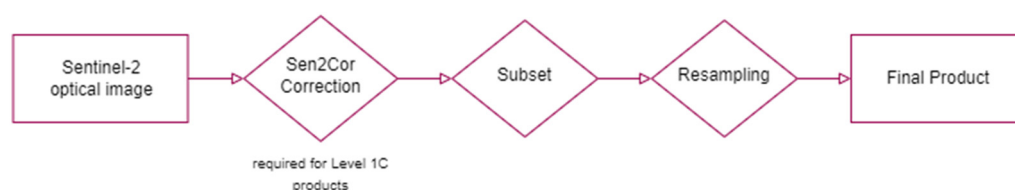

Figure 5. Pre-processing workflow of optical images.

3.4. Landcover Classification

The classification methodology of this study consists of two main parts, the analysis conducted in Sentinel-1 and Sentinel-2 products individually and the synergetic use of optical and radar data.

Random Forest and Maximum Likelihood supervised machine learning algorithms are utilised to classify the images. Maximum Likelihood classification determines the likelihood that a given pixel belongs to a certain class under the assumption that the statistics for each class in each band are normally distributed. [33]. In addition, the Random Forest classifier uses different data subsets of both the input bands and the training pixels, to determine the most reliable thresholds based on the input features with the highest prediction importance [34].

Multi-sensor image fusion techniques combine two or more geometrically registered images of the same scene into one single image that is more easily interpreted than any of the originals. Existing fusion techniques combine data from various sensors to take advantage of their complementary information content, generally at the pixel level. The following section consequently explores the combination combination of SAR and optical features to examine if the feature fusion of Sentinel-1 and 2 can improve the accuracy of the urban mapping method and in order to select the optimal algorithm based on the experiments conducted. For this reason, urban and vegetation indices were also computed. Specifically, the Index-based Built-up Index (IBI), Normalised Difference Built-up Area Indicator (NDBI), Urban Index (UI), and Normalized Difference Vegetation Index (NDVI) were all used in the process. The IBI, NDBI, and UI are indices for quickly mapping built-up areas. In contrast, the NDVI is a well-known spectral index for mapping vegetation distribution and various conditions over land surfaces. In the past, though, the NDVI was also applied for mapping the impervious area of urban areas. As the Modified Normalised Difference Water Index (MNDWI) is suitable for enhancing open water features and extracting water bodies, it was applied here in the analysis of the project area in Limassol. In the presented process, the spectral indices were calculated by the classification process. All the source bands were used in this step, including the ratio band created by the SAR image and the spectral indices. Numerous experiments were carried out to discover the most accurate and suitable combination of indices.

One of the most fundamental parts of the classification process is the collection and analysis of training samples. During the selection process of the training areas, the Open Street Map labelled datasets were utilised, as well as land cover data provided by the Cyprus Department of Lands and Surveys, which were used as guided maps. In the presented case, the training data were grouped into three main categories (buildings, vegetation, and water) based on the city's urban structure and the scope of the study. These groups were categorised in the QGIS environment [35] for processing flexibility and future management of geodata. This includes cross-platform integration and open data provision, to ensure the results of this activity can be integrated into the online PERIsCOPE project platform.

3.5. Change Detection

According to Singh [36], change detection is the process of identifying differences in the state of an object or phenomenon by observing it at different times. Over the past decades, many detection techniques and methods have been developed in order to analyse the frequent environmental changes and overcome the challenges of particular environmental concerns. Lu et al. [37] state that change detection methods are grouped into seven categories: algebra, transformation, classification, advanced models, geographic information system (GIS) approaches, visual analysis, and other approaches.

Applying multi-looking and co-registration of the calibrated products results in the temporal images being connected and prepared for further analysis. In the case of SAR images, the SNAP change detection module is applied in the stacked output. The SNAP change detection tool is based on log-likelihood estimation, which is the difference between the log intensity estimates. In this way, the areas of major change were highlighted. The results were vectorised and displayed in the QGIS [36] environment. QGIS (v3.28.4) is an open-source geospatial software that views, edits, and analyses geographic information.

In the case of optical products, image differencing was applied, a widely used technique for many applications involving change detection. Close et al. [38] showed that image differencing achieves one of the highest overall accuracy scores (94%).

$$ChangeMap = \left(\frac{B_{2022} - B_{2016}}{B_{2022} + B_{2016}} \right)^2$$

where B corresponds to the different bands of Sentinel-2 images ($B2$, $B3$, $B4$, $B5$, $B6$, $B7$, $B8$, $B11$ and $B12$) of the collocation of 2016 and 2018 images. In this equation, the normalised squared difference was applied, which rescales the values into a range of 0 to 1. The normalised squared difference facilitates thresholding since it regroups the change pixels distributed initially in the tails of the distribution curve around the mean to a unique direction. After comparing the differences between the various bands, B8 was selected. Once the created index is differenced, the resulting image values are then thresholded to identify areas of change.

4. Results

The results of this study are presented here in two parts. The first part describes the land cover classification outputs in the areas of interest, and the second part deals with the change detection in the urban regions.

4.1. Land Cover Analysis

It is necessary to compare the two supervised machine learning approaches to determine the most effective in the areas under study. In addition, Sentinel-2 images were included in this procedure to achieve the finest results possible. The final classified images and the detailed outcomes of the algorithms are presented in Figures 6 and 7 for both urban areas under study.
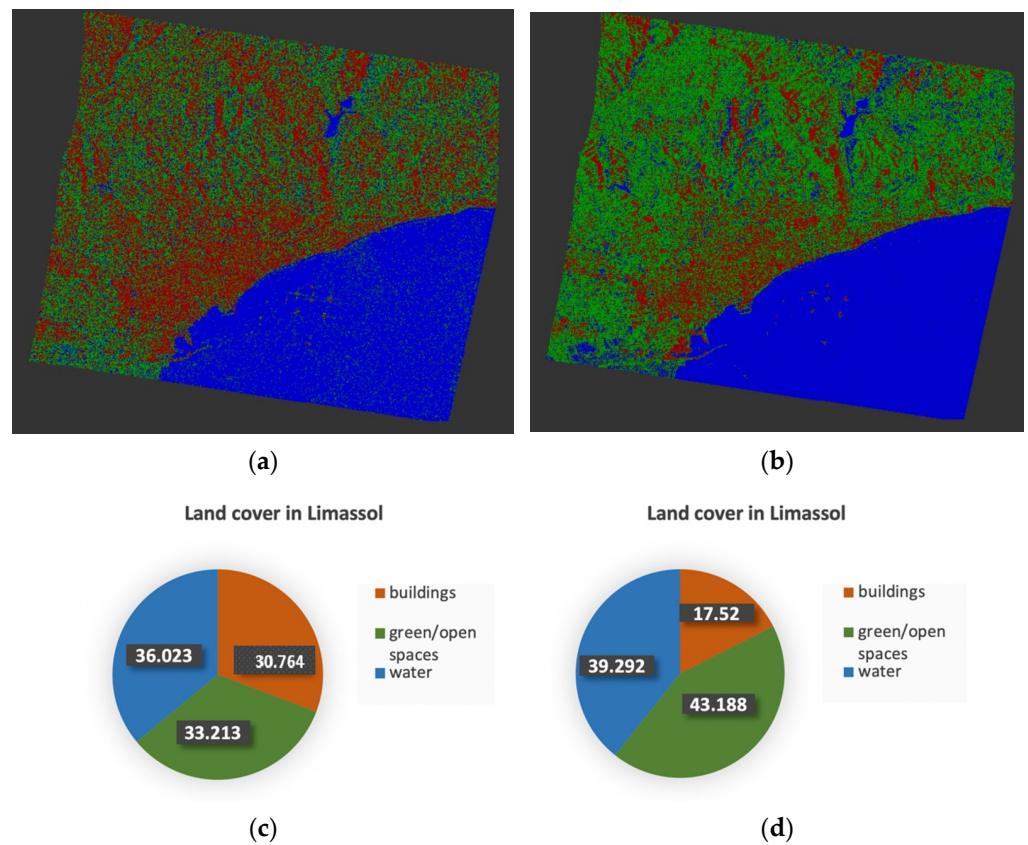
(a)　　　　　　　　　　　　　　　**(b)**

Land cover in Limassol　　　　　　　　　Land cover in Limassol

(c)　　　　　　　　　　　　　　　**(d)**

Figure 6. Comparison of Supervised Classifiers in Limassol: (**a**) Result of Random Forest Classifier; (**b**) Result of Maximum Likelihood Classifier; (**c**) Percentage of Land Cover—RF; (**d**) Percentage of Land Cover—M.

(a)　　　　　　　　　　**(b)**　　　　　　　　　　**(c)**

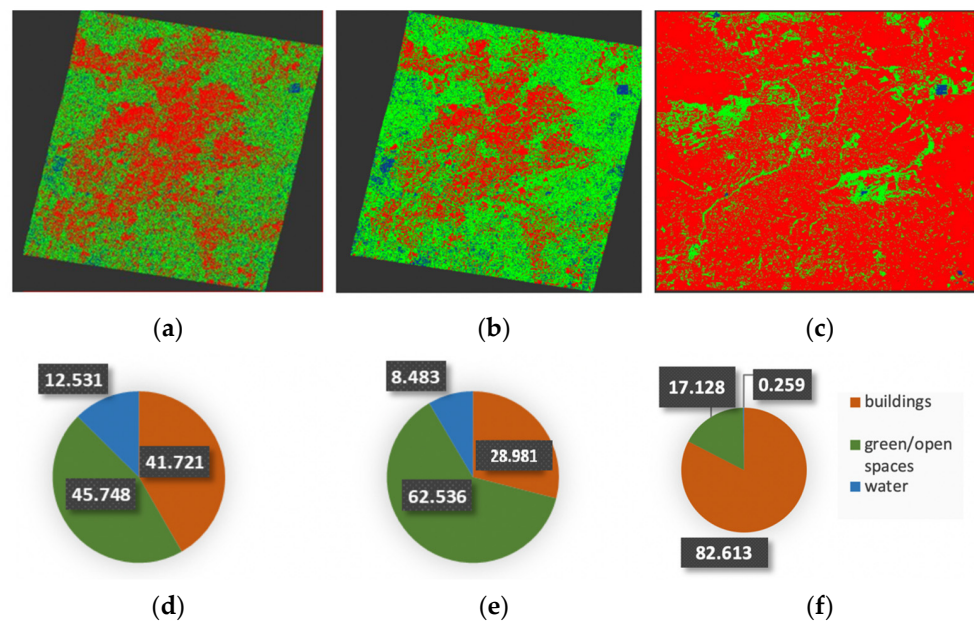**(d)**　　　　　　　　　　**(e)**　　　　　　　　　　**(f)**

Figure 7. Comparison of Supervised Classifiers in Nicosia: (**a**) Random Forest—Sentinel-1; (**b**) Maximum Likelihood—Sentinel-1; (**c**) Random Forest—Sentinel-2; (**d**) Land Cover—RF; (**e**) Land Cover—ML; (**f**) Land Cover—S2/RF.

According to the evaluation of the classifiers, the Random Forest algorithm performs better than the Maximum Likelihood algorithm, especially for the urban category. The

overall accuracy of 85.01% manifests how well the training data was classified, based on the hierarchical thresholding of the Random Forest.

In the case of Nicosia, the Random Forest classifier was also applied in Sentinel-2 optical products, using the 2nd, 3rd, 4th, 8th, 11th, and 12th bands. It is concluded that the Random Forest algorithm utilised in Sentinel-2 produces the best results based on the visual interpretation of the classified images (Figure 6) and the evaluation of the methods. Table 2 presents the different accuracy metrics for the three trained classes.

Table 2. Training accuracy metrics for the three classifiers.

	Buildings			Open/Green Spaces			Water		
	RF-S1	**ML-S1**	**RF-S2**	**RF-S1**	**ML-S1**	**RF-S2**	**RF-S1**	**ML-S1**	**RF-S2**
accuracy	0.794	0.845	0.940	0.692	0.744	0.925	0.819	0.881	0.980
precision	0.707	0.846	0.930	0.570	0.611	0.915	0.688	0.831	0.970
correlation	0.646	0.702	0.886	0.537	0.602	0.860	0.630	0.730	0.866
error rate	0.206	0.155	0.060	0.309	0.256	0.074	0.181	0.120	0.020
True Positives	727	695	947	572	782	919	520	572	154
False Positives	302	127	80	432	497	86	236	116	7
True Negatives	1487	1662	1113	1357	1292	1107	1764	1884	1993
False Negatives	273	305	52	428	218	80	269	217	38

During the procedure of joint use of Sentinel-1 and Sentinel-2 data, various combinations of source bands and spectral indices were performed. It is concluded that in the case of Limassol, the finest classification output was achieved with the use of all radar and optical bands and also the NDBI, IBI, NDVI, UI, and MNDWI indices. Based on the classifier evaluation, the overall accuracy equals 90.40%. The output demonstrates that the synergetic methodology outperforms Limassol, as the percentage is higher by 5%. The classification output is displayed in Figure 8.
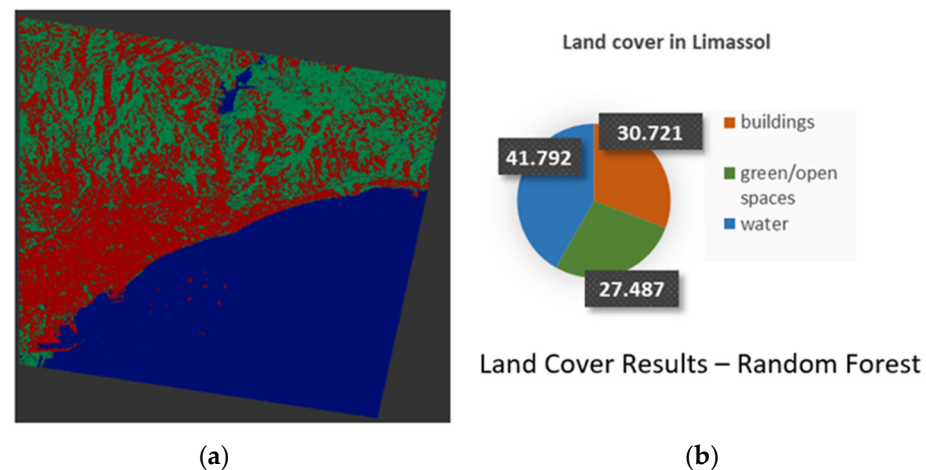

| (**a**) | (**b**) |

Figure 8. Classification Results in Limassol from the synergetic use of SAR and optical data: (**a**) Random Forest output; (**b**) Land Cover.

Based on the assessment and the interpretation of the classification maps, the Random Forest algorithm is applied on all radar and optical bands, while the NDBI, IBI, NDVI, and UI spectral indices deliver the optimal outcome. This combination achieved an overall accuracy of 94.10%. The high accuracy of the classifier compared to the previous results in the case of Nicosia (91%), indicated that the joint use of Sentinel-1 and Sentinel-2 products achieves the highest performance—Figure 9 provides the classified image. The most accurate classification maps were used in the following steps.
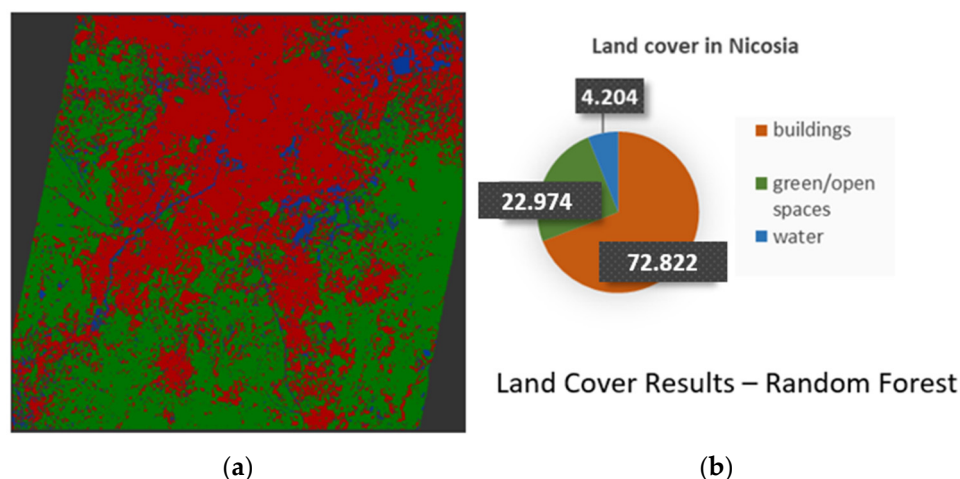
(**a**)　　　　　　　　　　　　　　　　　　　　(**b**)

Figure 9. Classification Results in Nicosia from the synergetic use of SAR and optical data: (**a**) Random Forest output; (**b**) Land Cover.

4.2. Change Detection

Multi-temporal colour composite images can be used to visualise the land usage of an area. This method uses images of different dates to construct a colour composite that produces an image which displays features changing through time as various colours, while areas of no change are displayed as grey tones. Specifically, the red color in the images indicates the changes that occurred over the period of coverage. This step is useful to better understand the changes that occurred. For example, Figure 10 displays the RGB composite, and therefore the locations of Nicosia that changed between 2016 and today.
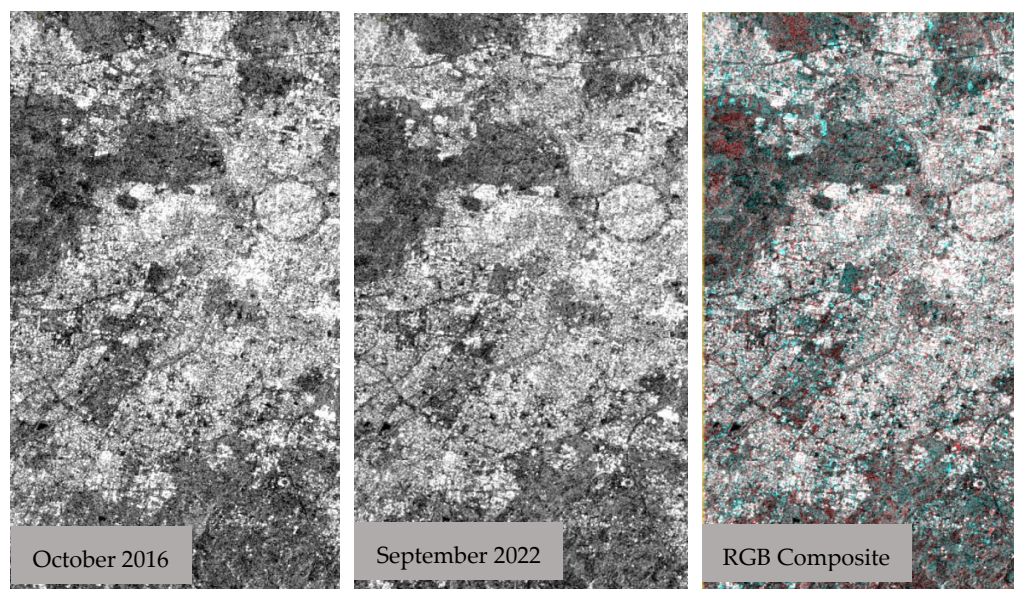

Figure 10. Visualization of Changes in Nicosia—RGB Composite.

The following step is the change detection tracking in SAR images. The procedure includes implementing the change detection SNAP module in the created stack containing the corrected radar images of 2016 and 2019. The result is a ratio band, which indicates the differences in the dB values from the before and after images. Figure 11 shows the visualisation of the changed pixels in Google Earth. The detected changes are marked in the figure in red.

Figure 11. Changes tracked in SAR images visualized on Google Earth: (**a**) Limassol; (**b**) Nicosia.

To enrich the results, change detection techniques in Sentinel-2 images were also applied. The normalised squared difference was performed in the areas under study in Nicosia and Limassol, and the outputs were extracted as Geotiffs and KML file formats. The tracked changes in both cities on the Google Earth environment are illustrated in Figure 12. In the case of Limassol, the pixels that correspond to the sea were removed for the algorithm to focus on the city's urban fabric.

Figure 12. Changes tracked in optical images visualized on Google Earth: (**a**) Limassol; (**b**) Nicosia.

Subsequently, output data were transferred from SNAP into the QGIS environment as a GeoTIFF file for post-processing to generate valuable urban change detection maps. Open Street Map was used as the base map for the representative visualisation of the results. The vectorisation of the raster data was considered necessary to overlay the changed parts with the corresponding classified images. As a result, the changes were then categorised, and areas of the built environment that changed the most over the past six years were highlighted. Figure 13 shows a change detection map of Nicosia and Limassol produced by SAR data, and combined with the classification results. Figure 14 illustrates the changes generated by optical data in both cities.

As indicated in both Nicosia and Limassol, the areas with noticeable differences in the readings are detected in the class of buildings. This fact confirms the dynamic of urban growth, as described in previous sections. In addition, it is clear that the percentage of tracked changes obtained from the SAR images is higher. This fact confirms the conclusion of Li et al. [12] that multi-temporal SAR images are the most suitable choice for change detection applications.

In the context of PERIScOPE, the historic cluster of Strovolos in Nicosia and the Turkish-Cypriot quarter of Limassol were selected as the testbed areas for further, focused analysis. Figure 15a displays a map that visualises changes in the Strovolos area and the land cover layer. The identified changes in Strovolos' surrounding environment can be interpreted from the expansion and transformation of the region over the past few years. In addition to residential uses, the area was recently transformed into a semi-commercial centre.
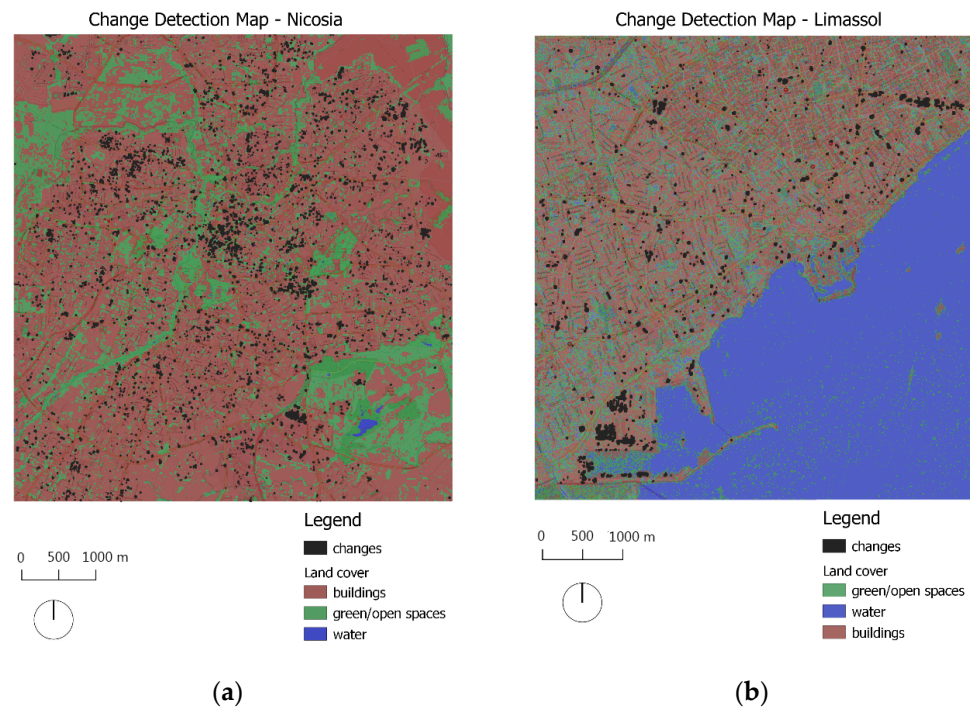
Change Detection Map - Nicosia

Change Detection Map - Limassol

Legend

changes

Land cover

buildings

green/open spaces

water

0   500 1000 m

Legend

changes

Land cover

green/open spaces

water

buildings

0   500 1000 m

(**a**)

(**b**)

Figure 13. Change detection maps produced by SAR data wherein polygons of changes are overlaid with the classification results: (**a**) Nicosia; (**b**) Limassol.
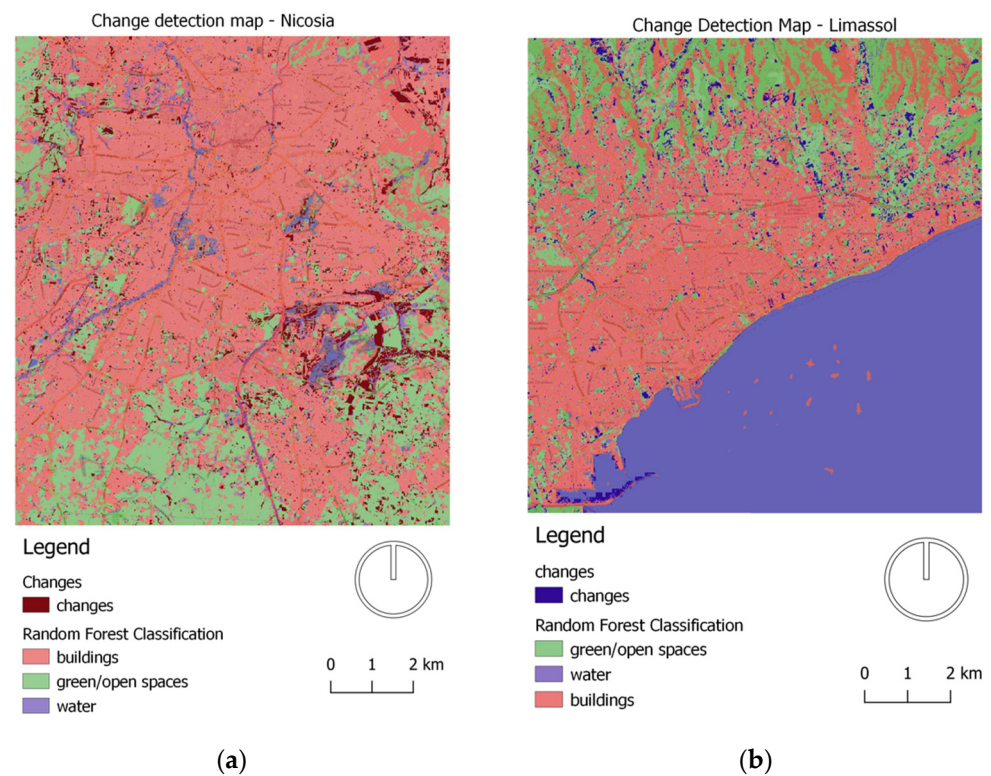
Change detection map - Nicosia

Change Detection Map - Limassol

Legend

Changes

changes

Random Forest Classification

buildings

green/open spaces

water

0   1   2 km

Legend

changes

changes

Random Forest Classification

green/open spaces

water

buildings

0   1   2 km

(**a**)

(**b**)

Figure 14. Change detection maps produced by optical data wherein polygons of changes are overlaid with the classification results: (**a**) Nicosia; (**b**) Limassol.
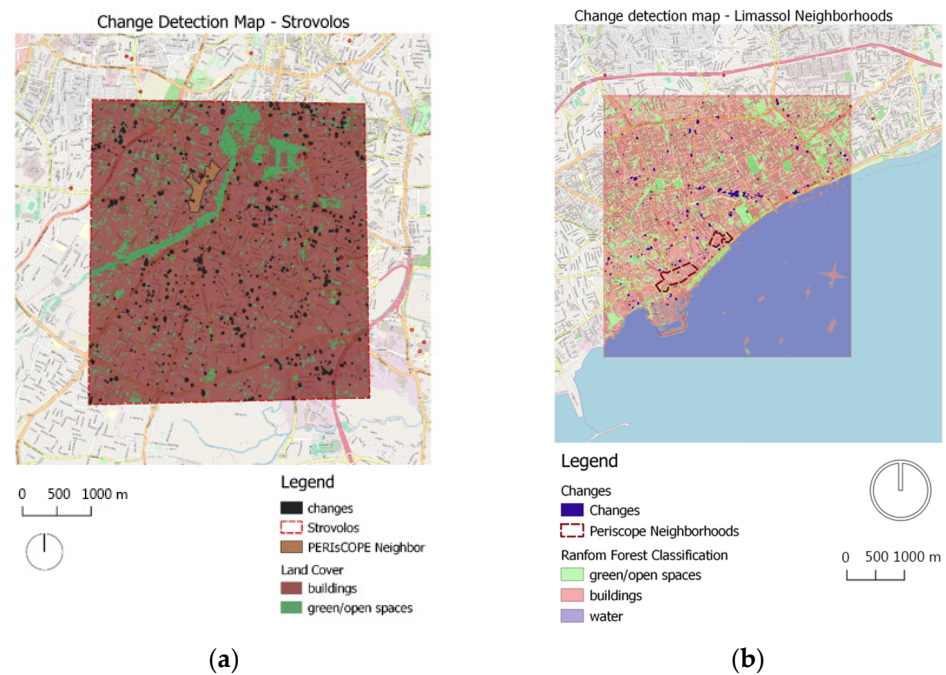
Figure 15. Focused analysis of the study areas by means of change detection maps of (**a**) Strovolos; (**b**) the Turkish-Cypriot quarter of Limassol.

In the Limassol neighbourhoods, the classification analysis was conducted again with the joint use of radar and optical data to detect the borders between the Limassol Marina and the sea in detail. 93% overall accuracy was achieved. In that case, the change detection was performed in SAR data, implementing the SNAP change detection tool. Fewer changes were tracked that were interpreted as typical built environment changes through new building construction and the creation of the marina of Limassol, cf. Figure 15b.

As the final results of this study are expected to be integrated into the PERIsCOPE platform, it was required to convert the research outputs into two-dimensional georeferenced data, as well as to generate their three-dimensional representations. The 3D maps provide a realistic representation of the tracked changes that professionals and city stakeholders may use. Figure 16 displays a screenshot of the change detection 3D map of Limassol.

Figure 16. 3D change detection map of Limassol.

The authors envision that using chronological series of satellite images to understand changes in the built environment over time can help to better inform relevant city authorities about urban fabric transformations and identify possible threats. This insight can thus be valued as a useful tool that contributes to the sustainable management of a city.

5. Discussion

In this study, the classification results were derived from supervised machine learning algorithms, such as the Random Forest and the Maximum Likelihood classifier. This kind of approach demands labelled data to predict outcomes. However, obtaining an adequate amount of data might be a challenge for researchers. For instance, in this study, the supervised algorithms could not be utilised on 2016 images due to the limited availability of OpenStreetMap land cover data from that year. In this case, unsupervised machine learning algorithms could be applied. The study presented how unsupervised learning can identify hidden patterns or intrinsic structures in the data, and can be used to draw conclusions from datasets composed of unlabelled input data. Specifically, in this research process step, the k-means algorithm was applied, which assigns each data point to the cluster whose centre is closer [39]. The k-means classifier was selected as it is one of the most widely used unsupervised algorithms. Figure 17 displays the result of k-means classification in Nicosia, as applied in both Sentinel-1 and Sentinel-2 images. Thirty iterations and three clusters were chosen as the parameters of the algorithm. As can be noticed, the outputs of the k-means analysis are imprecise. For instance, in the radar image, the water bodies of Nicosia were not detected, and in the optical image, water class covers 22.286% of the region of interest, which is not valid. The study showed that supervised Random Forest and Maximum Likelihood classification could be much more accurate than unsupervised k-means classification, but unsupervised classification is particularly useful when data or prior knowledge about the study area is unavailable.
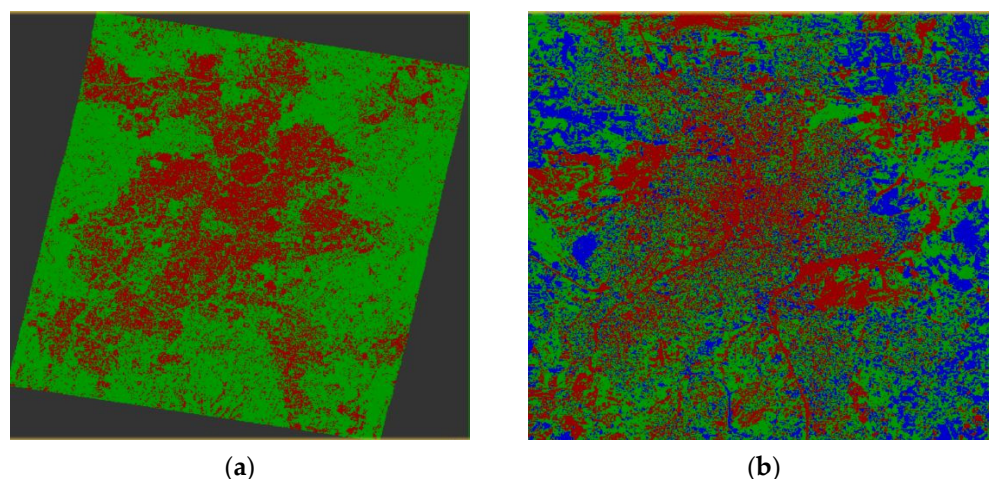

(**a**)   (**b**)

Figure 17. K-means unsupervised classification results in Nicosia as applied in (**a**) Sentinel-1; (**b**) Sentinel-2.

The next steps in the development of the research comprise the integration of the QGIS datasets delivered by this process into the PERIsCOPE platform (Figure 18). More specifically, the results will be available in GeoTIFF format, downloadable, and also visualised in interactive maps. Future research on this topic includes the integration of the presented methodology as a tool into the content management system that supports the PERIsCOPE platform. In the future, this tool will facilitate the identification of multitemporal changes in the vicinity of heritage building clusters based on satellite images in an online, user-friendly environment. Combined with land surface temperature maps [38] of the areas under study, the authors envision this tool becoming a valuable support mechanism for data interpretation and decision-making in heritage management and building conservation processes.
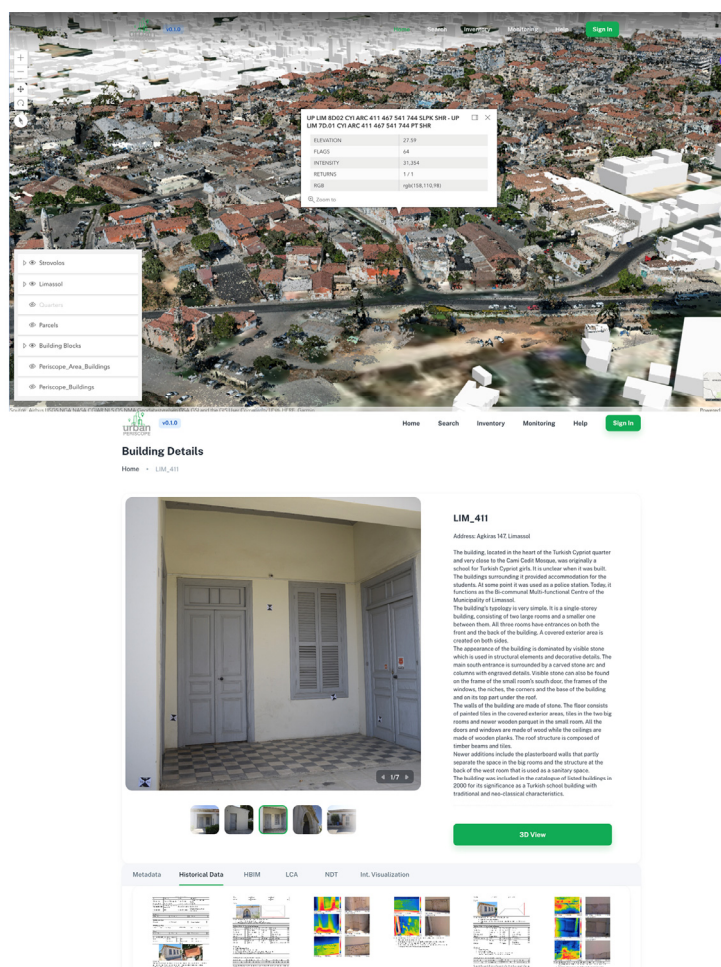
Figure 18. Data visualization of Strovolos historical core on the alpha version of the online PERIsCOPE platform.

6. Conclusions

The aim of this study was to present a methodology for change detection in urban environments with the employment of supervised machine learning algorithms. Additionally, the performance of the synergetic use of radar and optical data was examined. Specifically, the Sentinel-1 SAR images were combined with Sentinel-2 images, indicating that a significant improvement in land cover classification accuracy can be achieved, compared to the case where only optical or radar imagery is used. The temporal analysis was conducted for the time period 2016–2019 for two Cypriot cities – Nicosia and Limassol – and the required Sentinel-1 and Sentinel-2 images were acquired by the European Space Agency's (ESA) Copernicus Hub. The entire processing workflow was completed on the SNAP environment – a tool used for Earth Observation analysis. The study's results deliver information concerning the cities' expansion trends, simultaneously mapping the urban landscape changes and dynamics.

The main contribution of this study concerns the evaluation of a workflow that can be used in the built environment of historic clusters in Cypriot cities, to enable authorities to monitor the urban fabric of sensitive areas threatened by climate decay through the PERIsCOPE platform. Here, 'monitoring' is used in terms of a process that enabled the study and observation of the built environment as a multifactorial topic, since it employs a two-part approach that includes classification and change detection analysis. Furthermore, this study contributes to field of sustainable and energy efficient heritage-built environment, as it provides the ground for analysis related to the urban heat island effect. The development and delivery of tools, which allow for the comprehensive investigation

of changes in urban density and spatial planning, establishes the conditions for detailed insights into parameters that affect the city microclimate. The value-adding service of the PERIsCOPE HBIM platform, presented in this study, delivers new perspectives for HBIM tools Supplementary Material S1, enabling the combination of information in different layers, towards a more energy-efficient built environment.

The presented workflow and methods are applied as a pilot in the analysis of vulnerable historic clusters in Cypriot cities that face rapid urbanisation challenges and the impact of climate change. However, the research can also be applied to other historical city regions, using the technical guidelines, workflows, and instructions delivered under the context of this study. The potential of promoting heritage reuse and safeguarding as a pillar of socio-economic growth and sustainable development is gaining acknowledgment by policymakers and decision-makers. This study addresses the need for agile digitisation and open access to comprehensive information resources for building energy upgrades.

Supplementary Materials: The following supporting information can be downloaded at: S1: https://youtu.be/lFMau9XZrKs (accessed on 12 February 2023) [alpha version of the UPERIsCOPE platform]; S2: https://youtu.be/tFZ_aDuhWw8 (accessed on 18 January 2023) [data fusion].

Author Contributions: Conceptualization, G.A. and M.S.T.; methodology, A.A., C.C. and P.F.; software; validation; formal analysis; investigation; resources; data curation, M.S.T., A.A. and C.C.; writing—original draft preparation, M.S.T. and G.A.; writing—review and editing, A.A., C.C., V.L. and P.F.; visualization, M.S.T.; supervision, G.A.; project administration, funding acquisition, G.A. All authors have read and agreed to the published version of the manuscript.

Data Availability Statement: Sample datasets of satellite analysis and one pilot building supporting this study's findings are openly available in Zenodo at https://doi.org/10.5281/zenodo.7426346 (accessed on 21 February 2023); https://doi.org/10.5281/zenodo.7404274 (accessed on 21 February 2023), respectively. Further datasets supporting this study's findings are openly available in the UPERIsCOPE platform at https://uperiscope.hpcf.cyi.ac.cy/ (accessed on 20 March 2023).

Conflicts of Interest: The authors declare no conflict of interest.

References

1. Shahat, E.; Hyun, C.; Yeom, C. City Digital Twin Potentials: A Review and Research Agenda. *Sustainability* **2021**, *13*, 3386. [CrossRef]
2. Boulanger, S.O.M. The Roadmap to Smart Cities: A Bibliometric Literature Review on Smart Cities' Trends before and after the COVID-19 Pandemic. *Energies* **2022**, *15*, 9326. [CrossRef]
3. Yarashynskaya, A.; Prus, P. Smart Energy for a Smart City: A Review of Polish Urban Development Plans. *Energies* **2022**, *15*, 8676. [CrossRef]
4. Adibhesami, M.A.; Karimi, H.; Sharifi, A.; Sepehri, B.; Bazazzadeh, H.; Berardi, U. Optimization of Urban-Scale Sustainable Energy Strategies to Improve Citizens' Health. *Energies* **2023**, *16*, 119. [CrossRef]
5. Bakr, N.; Weindorf, D.C.; Bahnassy, M.H.; Marei, S.M.; EI-Badawi, M.M. Monitoring land cover changes in a newly reclaimed area of Egypt using multi-temporal Landsat data. *Appl. Geogr.* **2010**, *30*, 592–605. [CrossRef]
6. Pesaresi, M.; Gerhardinger, A. Improved Textural Built-Up Presence Index for Automatic Recognition of Human Settlements in Arid Regions with Scattered Vegetation. *IEEE J. Sel. Top. Appl. Earth Obs. Remote Sens.* **2011**, *4*, 16–26. [CrossRef]
7. Rong, T.; Zhang, P.; Jing, W.; Zhang, Y.; Li, Y.; Yang, D.; Yang, J.; Chang, H.; Ge, L. Carbon Dioxide Emissions and Their Driving Forces of Land Use Change Based on Economic Contributive Coefficient (ECC) and Ecological Support Coefficient (ESC) in the Lower Yellow River Region (1995–2018). *Energies* **2020**, *13*, 2600. [CrossRef]
8. Gago, E.J.; Etxebarria Berrizbeitia, S.; Pacheco Torres, R.; Muneer, T. Effect of Land Use/Cover Changes on Urban Cool Island Phenomenon in Seville, Spain. *Energies* **2020**, *13*, 3040. [CrossRef]

9. Chen, Y.; Weng, Q.; Tang, L.; Liu, Q.; Zhang, X.; Bilal, M. Automatic mapping of urban green spaces using a geospatial neural network. *GISci. Remote Sens.* **2021**, *58*, 624–642. [CrossRef]

10. Verde, N.; Patias, P.; Mallinis, G. A Cloud-Based Mapping Approach Using Deep Learning and Very-High Spatial Resolution Earth Observation Data to Facilitate the SDG 11.7.1 Indicator Computation. *Remote Sens.* **2022**, *14*, 1011. [CrossRef]

11. Liu, H.; Yang, M.; Chen, J.; Hou, J.; Deng, M. Line-constrained shape feature for building change detection in VHR remote sensing imagery. *ISPRS Int. J. Geo-Inf.* **2018**, *7*, 410. [CrossRef]

12. Luo, L.; Li, P.; Yan, X. Deep Learning-Based Building Extraction from Remote Sensing Images: A Comprehensive Review. *Energies* **2021**, *14*, 7982. [CrossRef]

13. Li, L.; Wang, C.; Zhang, H.; Zhang, B.; Wu, F. Urban building change detection in SAR images using combined differential image and residual u-net network. *Remote Sens.* **2019**, *11*, 1091. [CrossRef]

14. Papadomanolaki, M.; Verma, S.; Vakalopoulou, M.; Gupta, S.; Karantzalos, K. Detecting Urban Changes with Recurrent Neural Networks from Multitemporal Sentinel-2 Data. In Proceedings of the International Geoscience and Remote Sensing Symposium (IGARSS), Yokohama, Japan, 28 July–2 August 2019; pp. 214–217.

15. SNAP—ESA Sentinel Application Platform v9.0.0. Available online: http://step.esa.int (accessed on 15 December 2022).

16. Tsolakidis, I.; Vafiadis, M. Urban land cover mapping, using open satellite data. Case study of the municipality of Thessaloniki. In Proceedings of the IOP Conference Series: Earth and Environmental Science, Changchun, China, 21–23 August 2020; IOP Publishing: Bristol, UK, 2020; p. 012062.

17. Radutu, A.; Sandru, M.I.V.; Nedelcu, I.; Poenaru, V.D. Change Detection trends in urban areas with remote sensing and socio-economic diagnosis in Bucharest city. In Proceedings of the International Multidisciplinary Scientific Geo Conference (SGEM, Sofia), Vienna, Austria, 7–10 December 2021; Volume 21.

18. Sundaram, S.; Yarrakula, K. Multi-temporal analysis of Sentinel-1 SAR data for urban flood inundation mapping—Cases tudy of Chennai Metropolitan City. *Indian J. Ecol.* **2017**, *44*, 564–568.

19. Simeone, D.; Rotilio, M.; Cucchiella, F. Construction Work and Utilities in Historic Centers: Strategies for a Transition towards Fuel-Free Construction Sites. *Energies* **2023**, *16*, 700. [CrossRef]

20. Chahardowli, M.; Sajadzadeh, H.; Aram, F.; Mosavi, A. Survey of Sustainable Regeneration of Historic and Cultural Cores of Cities. *Energies* **2020**, *13*, 2708. [CrossRef]

21. Agapiou, A. Estimating Proportion of Vegetation Cover at the Vicinity of Archaeological Sites Using Sentinel-1 and -2 Data, Supplemented by Crowdsourced OpenStreetMap Geodata. *Appl. Sci.* **2020**, *10*, 4764. [CrossRef]

22. Iranmanesh, R.; Pourahmad, A.; Faress, F.; Tutunchian, S.; Ariana, M.A.; Sadeqi, H.; Aghel, B. Introducing a Linear Empirical Correlation for Predicting the Mass Heat Capacity of Biomaterials. *Molecules* **2022**, *27*, 6540. [CrossRef]

23. Roshani, G.H.; Hanus, R.; Khazaei, A.; Zych, M.; Nazemi, E.; Mosorov, V. Density and velocity determination for single-phase flow based on radiotracer technique and neural networks. *Flow Meas. Instrum.* **2018**, *61*, 9–14. [CrossRef]

24. Qing, W.; Xinmin, W.; Shuo, P. The three-dimensional molecular structure model of Fushun oil shale kerogen, China. *J. Mol. Struct.* **2022**, *2022*, 1255. [CrossRef]

25. Mohaidat, M.; Grantner, J.L.; Shebrain, S.A.; Abdel-Qader, I. Instrument detection for the intracorporeal suturing task in the laparoscopic box trainer using single-stage object detectors. In Proceedings of the 2022 IEEE International Conference on Electro Information Technology (eIT), Mankato, MN, USA, 19–21 May 2022; IEEE: Piscataway, NJ, USA, 2022; pp. 455–460.

26. Basili, R.; Danciu, L.; Carafa, M.M.C.; Kastelic, V.; Maesano, F.E.; Tiberti, M.M.; Vallone, R.; Gracia, E.; Sesetyan, K.; Atanackov, J.; et al. Insights on the European Fault-Source Model (EFSM20) as input to the 2020 update of the European Seismic Hazard Model (ESHM20). 2013. Available online: https://meetingorganizer.copernicus.org/EGU2020/presentation/EGU2020-7008 (accessed on 30 March 2023).

27. Kpienbaareh, D.; Sun, X.; Wang, J.; Luginaah, I.; Kerr, R.B.; Lupafya, E.; Dakishoni, L. Crop Type and Land Cover Mapping in Northern Malawi Using the Integration of Sentinel-1, Sentinel-2, and PlanetScope Satellite Data. *Remote Sens.* **2021**, *13*, 700. [CrossRef]

28. OpenStreetMap Service. Available online: https://www.openstreetmap.org/ (accessed on 15 December 2022).

29. Faizan, M. Radarsat-2 Data Processing Using SNAP Software. 2020. Available online: https://www.researchgate.net/publication/352934165_Radarsat-2_data_processing_using_SNAP_software (accessed on 17 January 2023).

30. Jiang, W.; Yu, A.; Dong, Z.; Wang, Q. Comparison and analysis of geometric correction. *Sensors* **2016**, *16*, 973. [CrossRef] [PubMed]

31. Santoso, A.W.; Bayuaji, L.; Sze, L.T.; Lateh, H.; Zain, J.M. Comparison of various speckle noise reduction filters on synthetic aperture radar image. *Int. J. Appl. Eng. Res.* **2016**, *11*, 8760–8767.

32. Raiyani, K.; Gonçalves, T.; Rato, L.; Salgueiro, P.; da Silva, J.R.M. Sentinel-2 Image Scene Classification: A Comparison between Sen2Cor and a Machine Learning Approach. *Remote Sens.* **2021**, *13*, 300. [CrossRef]

33. Richards, J.A. *Remote Sensing Digital Image Analysis: An Introduction*; Springer: Berlin, Germany, 1999; p. 240.

34. Breiman, L. Random Forests. *Mach. Learn.* **2001**, *45*, 5–32. [CrossRef]

35. QGIS Development Team. QGIS Geographic Information System. Open Source Geospatial Foundation Project. 2022. Available online: http://qgis.osgeo.org (accessed on 15 December 2022).

36. Singh, A. Change detection in the tropical forest environment of north eastern India using Landsat. In *Remote Sensing and Tropical Land Management*; Eden, M.J., Parry, J.T., Eds.; John Wiley and Sons: Hoboken, NJ, USA, 1986; pp. 237–254.

37. Lu, D.; Mausel, P.; Brondizio, E.; Moran, E. Change detection techniques. *Int. J. Remote Sens.* **2004**, *25*, 2365–2401. [CrossRef]

38. Close, O.; Petit, S.; Beaumont, B.; Hallot, E. Evaluating 1. The Potentiality of Sentinel-2 for Change Detection Analysis Associated to LULUCF in Wallonia, Belgium. *Land* **2021**, *10*, 55. [CrossRef]

39. Krishna, K.; Murty, M.N. Genetic K-means algorithm. *IEEE Trans. Syst. Man. Cybern. B Cybern.* **1999**, *29*, 433–439. [CrossRef]